

Using Ultrawide Field-Directed Optical Coherence Tomography for Differentiating Nonproliferative and Proliferative Diabetic Retinopathy

Mohamed Ashraf¹⁻³, Jennifer K. Sun^{1,2}, Paolo S. Silva^{1,2}, and Lloyd Paul Aiello^{1,2}

¹ Beetham Eye Institute, Joslin Diabetes Center, Boston, MA, USA

² Department of Ophthalmology, Harvard Medical School, Boston, MA, USA

³ Ophthalmology Department, Alexandria Faculty of Medicine, Alexandria, Egypt

Correspondence: Mohamed Ashraf, Beetham Eye Institute, Joslin Diabetes Center, One Joslin Place, Boston, MA 02215, USA. mohamed.elmasry@joslin.harvard.edu

Received: September 13, 2022

Accepted: November 25, 2022

Published: February 6, 2023

Keywords: ultrawide field imaging; diabetic retinopathy; neovascularization; optical coherence tomography; proliferative diabetic retinopathy

Citation: Ashraf M, Sun JK, Silva PS, Aiello LP. Using ultrawide field-directed optical coherence tomography for differentiating nonproliferative and proliferative diabetic retinopathy. *Transl Vis Sci Technol.* 2023;12(2):7. <https://doi.org/10.1167/tvst.12.2.7>

Purpose: To evaluate the ability of ultrawide field (UWF)-directed optical coherence tomography (OCT) to detect retinal neovascularization in eyes thought to have severe nonproliferative diabetic retinopathy (NPDR).

Methods: Retrospective study of 20 consecutive patients diagnosed with severe NPDR by clinical examination. All patients underwent UWF color imaging (UWF-CI) and UWF-directed OCT following a prespecified imaging protocol to assess the mid periphery, 15/32 (46.9%) eyes underwent UWF-fluorescein angiography (FA). On OCT, new vessels elsewhere (NVE) were defined when vessels breached the internal limiting membrane.

Results: A total of 32 eyes of 20 patients were evaluated. Of the 45 suspected areas of intraretinal microvascular abnormalities (IRMA) on UWF-CI, 38 (84.4%) were imaged by UWF-directed OCT, and 9/38 IRMA (23.7%) were NVE by OCT. Furthermore, UWF-directed OCT identified seven additional NVE in three eyes not seen on UWF-CI. This resulted in a change in diabetic retinopathy (DR) severity from severe NPDR to PDR in 8/32 eyes (25.0%). Among the 46.9% of eyes with UWF-FA, UWF-directed OCT agreed with the UWF-FA findings in 80% (12/15 eyes), missing only one peripheral NVE outside the UWF-OCT scanning area. Two eyes had subtle NVD that were not evident on UWF-directed OCT.

Conclusions: This pilot study suggests that UWF-directed OCT may help differentiate IRMA from NVE and detect unrecognized NVE in eyes with advanced DR in a clinical practice setting. Future prospective studies in larger cohorts could determine whether this rapid and noninvasive method is clinically relevant in determining NVE presence or retinopathy progression and complication risk.

Translational Relevance: UWF-directed OCT may offer a noninvasive alternative to detect NVE in eyes with DR.

Introduction

Proliferative diabetic retinopathy (PDR) is a leading cause of severe visual loss in patients with diabetes mellitus.¹ Direct comparisons of ultrawide field (UWF) color imaging (UWF-CI) and UWF-fluorescein angiography (FA) suggest that up to 25% of eyes with PDR are missed on UWF-CI alone.² However, UWF-FA is an invasive procedure with possible side effects such as nausea, hypotension, and

life-threatening anaphylaxis.³ It is relatively contraindicated in patients with renal impairment or pregnant and lactating women. There have been many publications describing the features of new vessels elsewhere (NVE) and at the disc (NVD) using optical coherence tomography (OCT) and OCT angiography (OCTA).⁴⁻⁷ Many of those studies have helped describe the appearance of NVE on both en-face imaging and B-scans.

Recently a novel imaging device that combines both the UWF scanning laser ophthalmoscope and an UWF directed OCT has been developed (Silverstone, Optos,

plc, Dunfermline, UK). This device acquires a 200° UWF color image spanning 80% of the retinal surface that can then be used to direct an OCT scan to any area of that image including the posterior pole, mid-periphery, or far periphery. This camera is an entirely new device and not a software update to the prior UWF cameras. This device has been used to identify peripheral retinal lesions, but its use in detecting PDR has not been extensively studied.^{8,9} Although there have been prior attempts to acquire OCT scans of the periphery using regular OCT cameras, the technique is labor intensive, requiring a high level of skill and an excessive degree of patient participation. Even then the ability to capture most far peripheral lesions is limited.¹⁰

The purpose of the current pilot study was to evaluate the ability of UWF-directed OCT to detect retinal neovascularization in eyes thought to have severe nonproliferative DR (NPDR) when used in a clinical setting. Using a standardized retinal imaging protocol, the mid-periphery was screened for possible NVE. In addition, areas with large intraretinal microvascular abnormalities (IRMA) were imaged if it fell outside the standard imaging protocol coverage.

Methods

This retrospective study evaluated consecutive diabetes patients with treatment-naïve severe NPDR who presented to a single physician retina clinic (MA) at the Beetham Eye Institute of the Joslin Diabetes Center from July 1, 2021, to April 1, 2022. This physician is highly experienced in grading DR with certifications as both a grader and an adjudicator for the Joslin Vision Network international teleoph-

thalmology program, the BEI Reading Center and numerous clinical trials. Graders at the Joslin Vision Network undergo extensive training, examination, and quality control in DR grading, and the agreement rates between graders for grading DR severity on UWF images is substantial (weighted kappa 0.88 to 0.93).¹¹ Patients with prior anti-VEGF injections, panretinal photocoagulation, or other significant non-diabetic retinal pathology were excluded. The study was approved by the institutional review board at the Joslin Diabetes Center.

All patients received on-axis, non-steered 200° UWF-CI (California, Optos, plc, Dunfermline, UK) before physician evaluation. If the physician evaluation of the UWF-CI resulted in a grade of severe NPDR, UWF-directed OCT was then performed with the integrated UWF retinal imaging and swept-source OCT device (Silverstone, Optos, plc, Dunfermline, UK). UWF-CI and UWF-directed OCT images were obtained using this machine as described below. OCT scans were acquired using 100,000 A-scans per second and the 1050 nm swept-source laser. A subset of patients underwent UWF-FA as part of standard care for possible PDR after their OCT scans were completed.

UWF-Directed OCT Imaging Protocol

The UWF-directed OCT was used to obtain a 14 × 9 mm raster protocol centered on the fovea (thus including the macula, optic disc, and superotemporal to inferotemporal arcades) and five peripheral volume scans (6 × 6 mm) encompassing all four quadrants and the nasal retina (Fig. 1). Each volume scan had 120 individual b-scans. The prespecified protocol was selected to cover the UWF areas of highest NVE frequency.^{12–14}

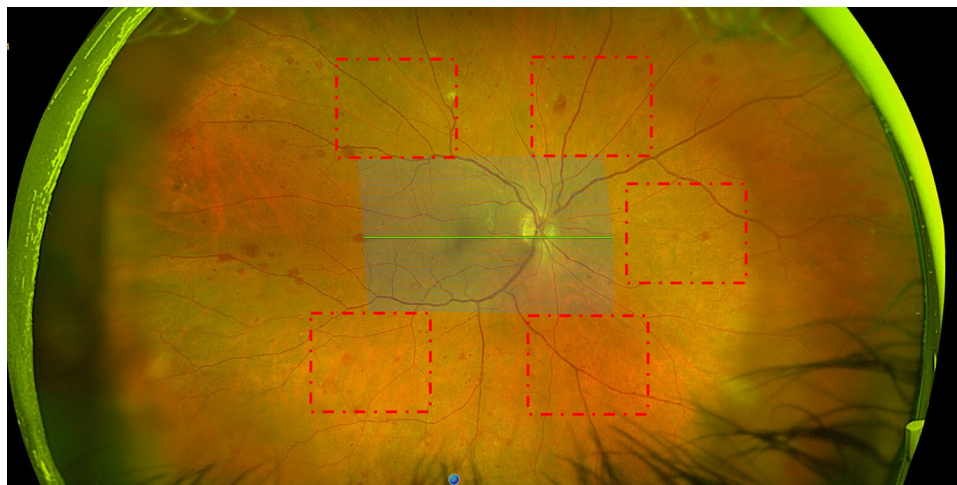


Figure 1. UWF-directed OCT scanning protocol used in eyes with severe nonproliferative diabetic retinopathy. In addition to a raster protocol that includes the macula, five additional mid-peripheral navigated scans (superotemporal, superonasal, nasal, inferonasal, and inferotemporal) are acquired for each eye (*dashed boxes*).

In addition, OCT was obtained for any area of IRMA greater than Early Treatment Diabetic Retinopathy Study standard photograph 8A that fell outside the standard imaging protocol. For the purpose of this study, if a single IRMA was larger than the cumulative size of all IRMA visualized on standard image 8A, then it was deemed suspicious. Of the 17,040 individual scans, 1031 (5.8%) were deemed unsuitable for analysis. On average the entire imaging protocol was less than three minutes per eye and can readily be acquired by technicians in a manner similar to that of standard OCTs.

Grading of NV on UWF-Directed OCT

Lesions were considered to be NV on OCT if retinal vasculature was observed to break through the internal limiting membrane.¹⁵ The classification described by Lee et al.¹⁵ was used to identify NVE or to distinguish them from possible IRMA (Supplementary Fig. S1). Briefly, IRMA were characterized by hyperreflective lesions in the inner retina (stage 1) or outpouching of ILM (stage 2) whereas NVE was characterized by disruption of the ILM (stage 1), horizontal growth along the posterior hyaloid (stage 2), multiple breaches of posterior hyaloid and linear growth (stage 3). Although challenging, NVE can be differentiated from vitreoretinal interface abnormalities by observing certain characteristics. NVE may or may not be continuous with the posterior hyaloid face. If continuous with

the posterior hyaloid face, they are present as areas of focal thickening and in some cases with anterior extensions into the vitreous. Furthermore, they do not block OCT signal in deeper retinal layers.

Results

The study included 32 eyes of 20 patients with diabetes and severe NPDR based on clinical assessment of UWF-CI. The mean age was 50.4 ± 13.9 years, 45% were female, 50% had type 2 DM, mean DM duration was 22.8 ± 8.3 years, and average HbA1c was $8.8\% \pm 1.8\%$.

A detailed list of all imaged eyes and the characteristics of individual lesions is presented in Supplemental Table S1. A total of 45 IRMA were suspicious for NVE on UWF-CI grading. Using the standard UWF-directed OCT imaging protocol, 38 of the 45 (84.4%) IRMAs were imaged. The remaining seven IRMAs failed to be captured using the standard imaging protocol because they were located outside the obtained volume scans. This occurred because the locations of the volume scans were placed manually by the imager with the possibility of overlap or unimaged spaces between the intended imaging areas. Among the IRMA imaged ($N = 38$), UWF-directed OCT determined that nine lesions (23.7%) in six eyes were actually NVE (Figs. 2 and 3). In addition,

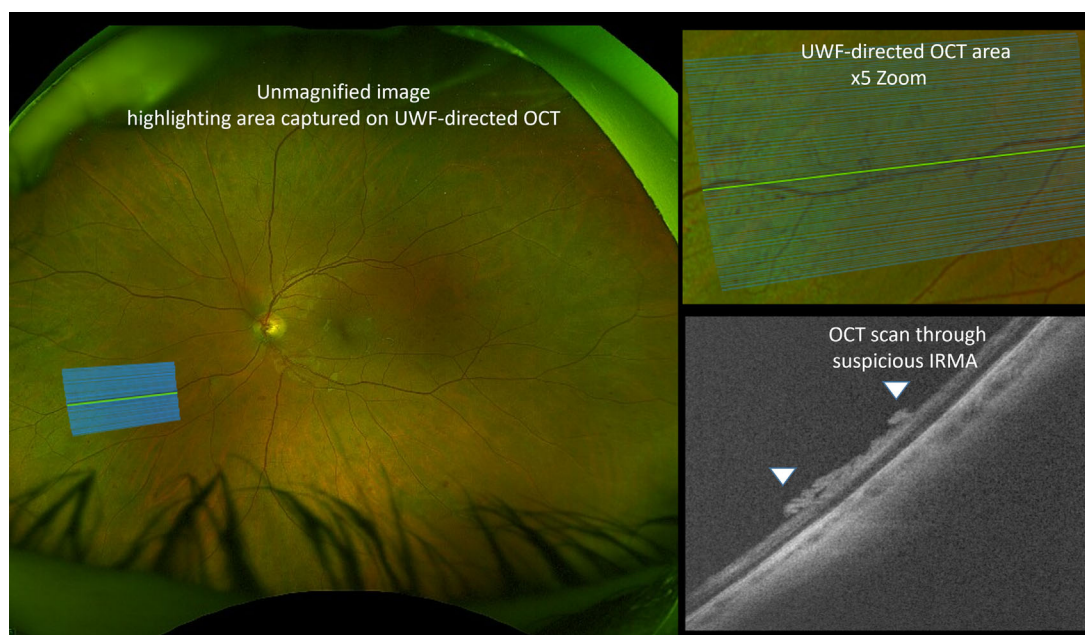


Figure 2. Example of an eye with areas of large IRMA that were confirmed to be NVE on UWF-directed OCT. Panel on the left shows an un magnified ultrawide field color image demonstrating the area where the UWF-directed OCT were acquired (*blue scans*). *Upper right panel* shows a magnified view of the area that was scanned highlighting large IRMA. *Lower right panel* shows the OCT results demonstrating neovascularization as it breaks through the internal limiting membrane (*white arrowheads*).

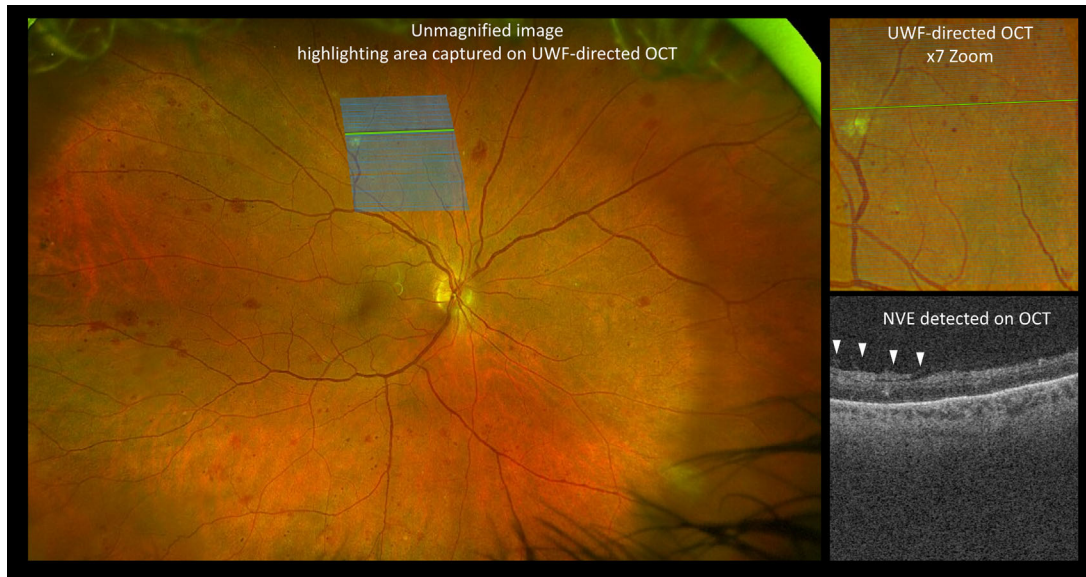


Figure 3. Example of an eye with a large IRMA that was confirmed to be NVE UWF-directed OCT. Panel on the left shows an un magnified ultrawide field color image demonstrating the area where the UWF-directed OCT were acquired (*blue scans*). *Upper right panel* shows a magnified view of the area that was scanned highlighting the large IRMA. *Lower right panel* shows the OCT results identifying neovascularization as it breaks through the internal limiting membrane (*white arrowheads*).

seven new NVEs in three eyes were detected using the prespecified midperipheral screening protocol that had not been previously suspected on UWF-CI alone (Figs. 4 and 5).

When assessing the morphology of the detected NVEs, three (16.7%) were small disruptions in the ILM (Lee et al.,¹⁵ stage 1), nine (50.0%) were flat and confined to the posterior hyaloid face (stage 2),

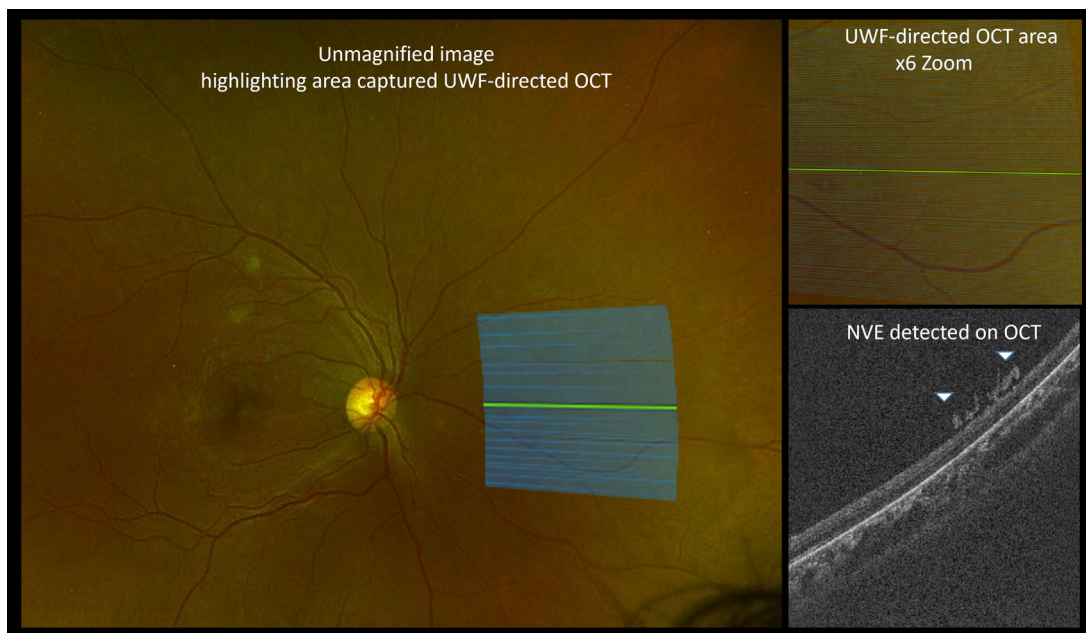


Figure 4. Example of an eye where using the standard sweeping protocol UWF-directed OCT detected previously unsuspected NVE. Panel on the left shows an un magnified ultrawide field color image demonstrating where the standard nasal OCT scans were acquired as per the protocol (*blue scans*) without neovascularization evident on the UWF color image. *Upper right panel* shows a magnified view of the area that was scanned showing no identifiable IRMA or NVE. *Lower right panel* shows the OCT results demonstrating neovascularization as it breaks through the internal limiting membrane (*white arrowheads*).



Figure 5. Another example of an eye where using the standard sweeping protocol for UWF-directed OCT detected previously unsuspected NVE. Panel on the left shows an unmagnified ultrawide field color image identifying the superotemporal area where OCT was acquired as per the imaging protocol (blue scans). Upper right panel shows the magnified UWF color image of the area that was scanned showing a highly visible choroidal blood vessels but no signs of IRMA or NVE. Lower right panel shows the OCT results demonstrating an area of neovascularization as it breaks through the internal limiting membrane (white arrowheads).

and six (33.3%) had anterior extension and vitreous invasion (stage 3). Overall, NVEs detected using UWF-directed OCT resulted in a change in the DR grade from severe NPDR to PDR in 8/32 eyes (25.0%).

As part of clinical care, 15/32 (46.9%) eyes underwent UWF-FA in addition to UWF-CI and UWF-directed OCT imaging. Among the subgroup of eyes with UWF-FA, UWF-directed OCT agreed with the UWF-FA findings in 80% (12/15). Two eyes had subtle NVD that were not evident on UWF-directed OCT. One eye had a small NVE in the far periphery of the nasal retina which fell outside the area covered by the UWF-directed OCT scanning protocol.

Discussion

This study demonstrates that the clinical use of UWF-directed OCT can detect NVE that might otherwise be considered IRMA or missed entirely by evaluation of UWF-CI alone. When imaging suspicious IRMA with OCT, approximately 24% were found to be NVE. In areas of the retina without suspicious IRMA or NVE on UWF-CI, seven NVEs in three eyes (9.4%) were detected using a standard UWF-directed OCT screening protocol. Overall, one quarter of eyes had a change in DR severity from severe NPDR to PDR based on UWF-directed OCT findings.

UWF-FA remains the gold standard in identifying NVE or NVD. In the current study, 46.5% (15/32) of eyes had both UWF-FA and UWF-directed OCT.

In this group there was exact agreement in the DR severity in 80% (12/15) of eyes. Two of the discrepant eyes had subtle NVD that was not evident on UWF-directed OCT, and one eye had a small peripheral NVE that fell outside the area covered by the UWF-directed OCT scanning protocol. OCT imaging of the optic nerve has a sensitivity of approximately 62% in detecting NVD compared to FA in eyes without a diagnosis of PDR.¹⁶ Thus additional studies are needed to assess the utility of UWF-directed OCT for NVD and whether altering scan density, identifying lesion specific features, or other factors may improve NVD detection.

Although the scanning protocol did not cover the entire retina, it was derived based on prior studies describing the location and distribution of IRMA and NVE on UWF imaging. Russell et al.¹² described the distribution of NVE in 651 eyes with PDR imaged with UWF-FA and reported that 99.4% of NVEs in treatment naïve eyes fell within a simulated WF-OCTA area with an average dimension of 22.1 × 21.6 mm or 4.49 disc to fovea lengths horizontally and 4.40 disc to fovea lengths vertically. Furthermore, the study reported that the two most common sites for NVE were the superotemporal (29.4%) and inferotemporal (25.6%) quadrants. The UWF-directed OCT imaging protocol used in the current study falls within the simulated widefield area previously described for OCTA and expands on it in the nasal and superior/inferior fields (Supplementary Fig. S2). Nevertheless, there are still areas of retina not imaged where NVE may be missed.

When developing a NVE imaging protocol there were two primary possible strategies: a prespecified protocol imaging area or a targeted approach imaging only suspected IRMA or NVE. Although both strategies have their merits, using a targeted approach may miss a substantial number of NVEs given that 43.8% (7/16) of NVEs detected were not suspected on UWF-CI. Furthermore, of the 45 suspected IRMAs, only 38 were able to be imaged (84.4%) because of challenges targeting some individual lesions given the non-magnified screen and the need to manually place volume scans. In contrast, among the 15 eyes that had UWF-FA in the current study, only one eye had an NVE that fell outside the image protocol (6%).¹² However, use of a defined protocol imaging area will need to balance acquisition efficiency with image area coverage.

Thus substantial further work is needed to refine the OCT imaging protocol area to ensure that the most NVEs are detected while minimizing acquisition time. Larger patient cohorts including UWF-FA will be required to confirm these pilot findings. Prospective studies would be required in the future to determine any added long-term clinical benefit of detecting subclinical peripheral NVE.

In conclusion, UWF-directed OCT can demonstrate that nearly 25% of suspected large IRMA are NVE. Furthermore, this approach can identify NVE that were not previously identified on UWF-CI. These data suggest that UWF-directed OCT may improve detection of PDR in eyes believed to have advanced NPDR. Future larger studies are needed to compare combined UWF-CI and UWF-directed OCT grading with UWF-CI grading alone and UWF-FA. In this way it can be established whether and in what ways the UWF-directed OCT approach may provide benefit over existing imaging modalities in current clinical practice. The development of a noninvasive method to readily assess overall retinal NVE burden may help predict the risk of diabetic retinopathy progression and could have significant clinical care benefits. However, until this can be demonstrated, FA remains the gold standard in detecting NV.

Acknowledgments

Supported by the Massachusetts Lions Eye Research Fund (Aiello, Sun, Silva, Elmasry) and the Joslin Diabetes Center (Diabetes Research Center [DRC] Enrichment Core and Clinical Research Center, grant number: P30DK036836). The Optos Silverstone was acquired through a Mass Lions Eye Research

Fund presidential grant (PI of the grant: Lloyd Paul Aiello). Optos had no role in the design or conduct of the study.

Disclosure: **M. Ashraf**, None; **J.K. Sun**, Adaptive Sensory Technologies (F), Boehringer Ingelheim (F), Genentech/Roche (F), Janssen (F), Physical Sciences Inc (F), NovoNordisk (F), Optovue (F); **P.S. Silva**, Optos (F), Optomed (F), Optos (R), Optomed (R), Novartis (R), Bayer (R), Roche (R); **L.P. Aiello**, Kalvista (C), Novo Nordisk (C), MantraBio (C), Ceramedix (C), Optos (F), Kalvista (I), Optos (R)

References

1. The Diabetic Retinopathy Study Research Group. Photocoagulation treatment of proliferative diabetic retinopathy. Clinical application of Diabetic Retinopathy Study (DRS) findings, DRS Report Number 8. *Ophthalmology*. 1981;88:583–600.
2. Abdelal O, Elmasry MA, Shokrollahi S, et al. Comparison of diabetic retinopathy (DR) severity identified on ultrawide field retinal images (UWF-RI) and ultrawide field fluorescein angiograms (UWF-FA). *Invest Ophthalmol Vis Sci*. 2019;60:1571–1571.
3. Yannuzzi LA, Rohrer KT, Tindel LJ, et al. Fluorescein angiography complication survey. *Ophthalmology*. 1986;93:611–617.
4. Kilani A, Werner JU, Lang GK, Lang GE. Optical coherence tomography angiography findings in proliferative diabetic retinopathy. *Ophthalmologica*. 2021;244:258–264.
5. Pichi F, Smith SD, Abboud EB, et al. Wide-field optical coherence tomography angiography for the detection of proliferative diabetic retinopathy. *Graefes Arch Clin Exp Ophthalmol*. 2020;258:1901–1909.
6. Vaz-Pereira S, Morais-Sarmiento T, Esteves Marques R. Optical coherence tomography features of neovascularization in proliferative diabetic retinopathy: A systematic review. *Int J Retina Vitreous*. 2020;6:26.
7. Arya M, Sorour O, Chaudhri J, et al. Distinguishing intraretinal microvascular abnormalities from retinal neovascularization using optical coherence tomography angiography. *Retina*. 2020;40:1686–1695.
8. Sodhi SK, Golding J, Trimboli C, Choudhry N. Feasibility of peripheral OCT imaging using a novel integrated SLO ultra-widefield imaging swept-source OCT device. *Int Ophthalmol*. 2021;41:2805–2815.

9. Lee WW, Muni RH. Single-capture ultra-widefield guided swept-source optical coherence tomography in the management of rhegmatogenous retinal detachment and associated peripheral vitreoretinal pathology [published online ahead of print May 26,2022]. *Br J Ophthalmol*, <https://doi.org/10.1136/bjophthalmol-2021-320149>.
10. Choudhry N, Golding J, Manry MW, Rao RC. Ultra-widefield steering-based spectral-domain optical coherence tomography imaging of the retinal periphery. *Ophthalmology*. 2016;123:1368–1374.
11. Silva PS, Dela Cruz AJ, Ledesma MG, et al. Diabetic retinopathy severity and peripheral lesions are associated with nonperfusion on ultrawide field angiography. *Ophthalmology*. 2015;122:2465–2472.
12. Russell JF, Flynn HW, Sridhar J, et al. Distribution of diabetic neovascularization on ultra-widefield fluorescein angiography and on simulated widefield OCT angiography. *Am J Ophthalmol*. 2019;207:110–120.
13. Pan J, Chen F, Chen D, et al. Novel three types of neovascularization elsewhere determine the differential clinical features of proliferative diabetic retinopathy. *Retina*. 2021;41:1265–1274.
14. Silva PS, Cavallerano JD, Sun JK, Soliman AZ, Aiello LM, Aiello LP. Peripheral lesions identified by mydriatic ultrawide field imaging: Distribution and potential impact on diabetic retinopathy severity. *Ophthalmology*. 2013;120:2587–2595.
15. Lee CS, Lee AY, Sim DA, et al. Reevaluating the definition of intraretinal microvascular abnormalities and neovascularization elsewhere in diabetic retinopathy using optical coherence tomography and fluorescein angiography. *Am J Ophthalmol*. 2015;159:101–110.e101.
16. Wang XN, Zhou J, Cai X, Li T, Long D, Wu Q. Optical coherence tomography angiography for the detection and evaluation of ptic disc neovascularization: A retrospective, observational study. *BMC Ophthalmology*. 2022;22:125.